

Adsorption of lead from water by thiol-functionalized SBA-15 silicas

Phuong Tran Thi Thu · Tam Truong Thanh ·
Hung Nguyen Phi · Sung Jin Kim · Vien Vo

Received: 6 November 2009 / Accepted: 30 January 2010 / Published online: 10 February 2010
© Springer Science+Business Media, LLC 2010

Abstract Thiol-functionalized mesoporous silicas have been synthesized by co-condensation of tetraethoxysilane and varying contents of 3-mercaptopropyltrimethoxysilane in acidic medium with the block copolymer Pluronic 123 as a structure directing agent. Adsorption of lead in aqueous solution on the synthesized materials has been investigated. The adsorption data are fitted to Langmuir isotherms and a maximum adsorption capacity calculated from the Langmuir equation can reach 0.19 mmol of Pb/g. The stoichiometric ratio of S: Pb being 1:1 has been obtained for every adsorbent. The effect of the pH on lead adsorption, and desorption of lead on the lead-loaded materials have been studied.

Introduction

Heavy-metal ions in the natural environment arise from both natural and anthropogenic sources, and can be harmful to human and living organisms. Among them, lead exhibits high toxic for both the environment and human health. Lead is present in the environment from urban wastes and industrial activities like the manufacture of storage batteries, painting pigments, ammunition, automobiles, cable coverings, radioactivity shields, caulking, and bearings [1, 2]. Although there are many traditional treatment methods such as precipitation, oxidation, reduction, electrochemical

treatment, reverse osmosis, solvent extraction, adsorption, ion-exchange, and evaporation to be used for the metal bearing effluents, adsorption has proved to be one of the most feasible, simple, selective, cost-effective, ease of operation, and high-efficient process for the removal of heavy metals from polluted sources. Up to now, numerous experimental studies on Pb²⁺ adsorption by clays [3, 4], activated carbon [5], activated phosphate [6], chitosan nanoparticles [7, 8], peat or peat resin [9, 10], sawdust [11, 12], condensed tannin resin [13, 14], biomass [15], steel slag [16], dry plants [17], rice hull ash [18], etc., have been published. However, improvement of methods to treat wastewater containing lead ions still arises.

The mesoporous materials with periodic organization of channels on the nanometer scale synthesized using an aqueous liquid–crystal-templating route have received much attention due to their useful properties, such as large surface area, porous diameter, and high order [19–23]. Recently, the design of mesostructured-based adsorbents for the removal of toxic heavy-metal ions from aqueous solutions is a subject that has been intensively investigated [24–28]. For this purpose, a variety of organic functional groups such as thiol, amine can be grafted or incorporated onto the surface of mesopore channels using ligand-functionalized organosilanes [29, 30]. Among a wide variety of organosilanes to be used in anchoring the functionality to mesoporous silicas, (3-mercaptopropyl)trialkoxysilane [(RO)₃Si(CH₂)₃-SH, where R = CH₃ or CH₂CH₃] also represents effective ligands because sulfur, a soft non-metal, readily forms a covalent bond with soft metals to the right of the d-block elements. The thiol-derivatized HMS, MCM-41, and SBA-15 materials were capable of quantitatively adsorbing Hg²⁺ from different types of waste streams [24, 31]. However, few papers have been reported on functionalized SBA-15 materials for adsorption of lead from

P. T. T. Thu · T. T. Thanh · H. N. Phi · V. Vo (✉)
Department of Chemistry, Quy Nhon University, 170 An Duong
Vuong Street, Quy Nhon City, Vietnam
e-mail: vovien@dng.vnn.vn

S. J. Kim
Division of Nano Sciences, Department of Chemistry, Ewha
Womans University, Seoul 120-750, Korea

water. In this work, we present a study on the lead adsorption on thiol-functionalized SBA-15 materials synthesized by using varying proportions of 3-mercaptopropyltrimethoxysilane as a thiol source.

Experimental

Thiol-functionalized SBA-15 samples were synthesized by the following procedure. 2 g of P123 ($\text{HO}(\text{CH}_2\text{CH}_2\text{O})_{20}(\text{CH}_2\text{CH}(\text{CH}_3)\text{O})_{70}(\text{CH}_2\text{CH}_2\text{O})_{20}\text{H}$) were added to 62.5 g of HCl 1.9 M with stirring. The mixture was heated to 40 °C and then to the mixture 3.84 g of tetraethoxysilane (TEOS) was added. The resulting mixture was stirring for 45 min before the addition of 3-mercaptopropyltrimethoxysilane (MPTMS). Different molar ratios of MPTMS/TEOS of 0.05, 0.10, 0.15, 0.20, and 0.30 were used in the initial mixtures. The reaction mixture was stirred for 20 h at 40 °C, and then aged in an autoclave at 100 °C for 24 h. The solid product was separated by filtration, and washed with water several times. The structure directing agent (P123) was removed by using ethanol extraction at 70 °C for 24 h. These obtained materials are denoted as SBA-15/SH-*x*, where *x* is referred as the molar ratio of MPTMS/TEOS in percentage.

X-ray diffraction (XRD) for the samples were measured on the Bruker D8 Advance diffractometer using Cu K α radiation ($\lambda = 1.5406 \text{ \AA}$). N₂ adsorption–desorption isotherms were obtained on ASAP 2010 at 77 K. Before the measurement, the samples were degassed at 100 °C for 6 h. Infrared (IR) were recorded on a Thermo Nicolet spectrometer. Transmission electron microscopy (TEM) and scanning electron microscopy (SEM) were recorded on JEOL JEM-2100F and JEOL 5410, respectively.

Different sets of batch experiments have been carried out to investigate the effect of lead loading on the contact time, the initial lead concentration, and the pH of the aqueous solution. Single runs were carried out by stirring 50 mg of the adsorbent in 20 mL of aqueous Pb(NO₃)₂ solutions at 30 °C. When the adsorption procedure completed, the solutions were filtered and the residual lead(II) ions concentrations were then analyzed for by using an atomic absorption spectrophotometer (PerkinElmer AAnalyst 800). The lead adsorption capacity was determined by the difference between the initial and final lead concentrations in the solution.

The recovery and reusability of the adsorbent material are an important parameter related to the application potential of adsorption processes. In this study, the lead desorption was carried out by stirring the lead-loaded samples in HCl solution, and the adsorption was established as the procedure for adsorption experiments above. Each adsorption and desorption cycle was allowed 120 min

of contact time and consecutive adsorption–desorption cycles were repeated using the same adsorbent in solutions containing adsorbent-lead(II) ions for achieving adsorption or desorption equilibrium. The lead-reloaded adsorbent, recovered from the HCl solutions, was washed repeatedly with deionized water to remove any residual desorbing solution and placed into lead solution for the next adsorption cycle.

Results and discussion

Adsorbent characterization

The porous structure of the synthesized samples has been studied by low-angle XRD. The patterns in Fig. 1 show an intense reflection (100) and one additional weak peak at higher angle (110) for SBA-15/SH-5, indicative of a two-dimensional hexagonal space group with high *p6mm* symmetry [32]. The samples containing higher MPTMS ratios exhibit a single reflection with a significant intensity decrease and peak broadening. These results can be attributed to the loss of mesostructured order of the material with increasing organic content. From these values, the hexagonal lattice parameters are calculated and reported in Table 1.

The pore size and periodicity in the mesostructure of SBA-15/SH-*x* materials were confirmed directly by transmission electron microscopy. The TEM image for a representative material, SBA-15/SH-15 exhibits a highly ordered hexagonal arrangement of mesopores (Fig. 2). Both the perpendicular and parallel channels relative to the longitudinal axis are observed. The approximate intercore spacing of 10 nm is close to the value calculated from the

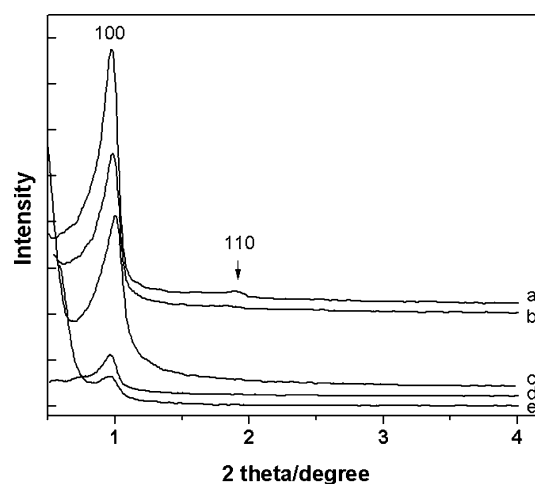
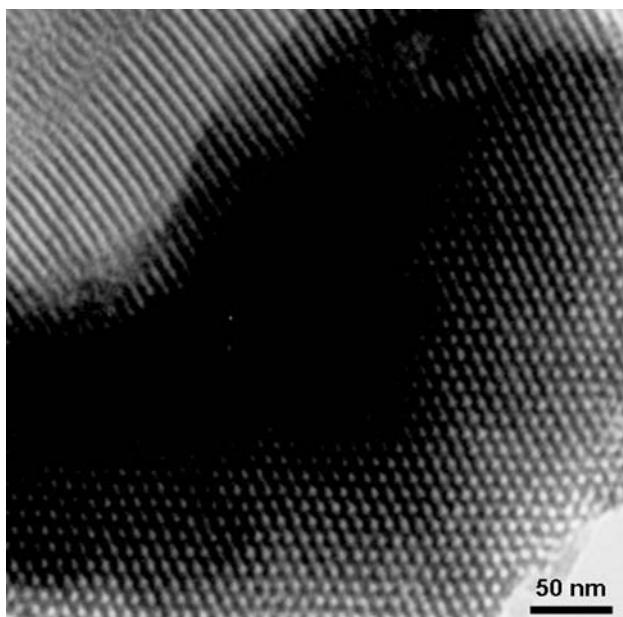


Fig. 1 Powder low-angle XRD patterns of the thiol-modified SBA-15 materials: SBA-15/SH-5 (a), SBA-15/SH-10 (b), SBA-15/SH-15 (c), SBA-15/SH-20 (d), SBA-15/SH-30 (e)

Table 1 Structural, textural properties of the thiol-functionalized SBA-15 materials

Material	S_{BET} (m ² /g)	Pore diameter (nm)	a_0 (nm)	Wall thickness (nm)
SBA-15/SH-5	720.7	6.1	10.5	4.4
SBA-15/SH-10	690.2	5.9	10.4	4.5
SBA-15/SH-15	582.3	5.0	10.2	5.2
SBA-15/SH-20	430.1	4.8	10.5	5.7
SBA-15/SH-30	210.2	3.9	10.6	6.7

**Fig. 2** TEM image of SBA-15/SH-15

XRD pattern, $a_0 = 10.2$ nm. The pore size and wall thickness, estimated from the HR-TEM image, are approximately 5.1 and 4.9 nm, respectively. The morphology of rope-like domains with a uniform size has been obtained for all the materials (Fig. 3). The particle sizes of 1.0, 0.7, 0.5, and 0.2 μm for SBA-15/SH-5, SBA-15/SH-10, SBA-15/SH-15, and SBA-15/SH-30, respectively, can be seen from the images. Interestingly, this indicates that particle size of the functionalized adsorbents decreases with increasing content of organic source.

The N_2 adsorption/desorption isotherms at 77 K as well as the calculated pore size distributions of thiol-functionalized SBA-15 samples are shown in Fig. 4. Characteristic mesoporous type IV IUPAC isotherms have been found for all samples. For the thiol-functionalized SBA-15 samples, it has been shown that isotherms with a capillary condensation of N_2 occurred over a slightly lower P/P_0 range and a slightly smaller pore volume in the functionalized samples with higher content of organic source. Generally, a change in the shape of isotherms and a broadening of the pore size distribution are observed when thiol functionalization increases. Pore diameter, pore volume, and superficial area BET (S_{BET}) are also found to decrease significantly with

increasing sulfur content. Conversely, silica wall thickness extracted from the XRD and nitrogen sorption parameters steadily increases in the same order (Table 1). These results can be attributed to the occupancy of propylthiol groups into the mesostructure. The above physisorption data indicate the presence of thiol groups, and the textural properties of SBA-15 were significantly maintained, showing a suitable porosity to act as lead adsorbents.

The incorporation of thiol groups in the silicate frameworks can be qualitatively confirmed by the FTIR data shown in Fig. 5. For the as-synthesized sample, the absorbance peaks corresponding to the C–H stretching and bending vibrations appear in the range of 2850–3000 and 1460 cm^{-1} , respectively. Those at 1377 and 1350 cm^{-1} are assigned to the stretches of C–O–C on P123 [33]. In addition, the typical Si–O–Si bands around 1220, 1070, 801, and 473 cm^{-1} associated with the formation of a condensed silica network are present. It is worth to note that a peak around 2570 cm^{-1} may correspond to vibrational mode of SH group [3]. For seeing more clearly, the IR curve was focused in the range 2400–2750 cm^{-1} , and showed in the inset of Fig. 5. An increase in intensity of this band for the materials with increasing organic content has been obtained. These results evidence strongly the presence of thiol groups and effect of MPTMS ratios on thiol group content on the functionalized SBA-15 materials.

Lead adsorption

Before doing the lead adsorption experiments on the thiol-functionalized SBA-15 samples, a test on lead adsorption in water for a pure as-synthesized SBA-15 sample was carried out. The result showed that the lead adsorption on the SBA-15 silica sample was negligible, so lead loading on the functionalized SBA-15 samples can be significantly attributed to the presence of thiol groups anchored to the silica mesostructure.

Adsorption equilibrium time

To obtain the equilibrium time of adsorption at 30 $^\circ\text{C}$, liquid-phase adsorption experiments were conducted on solutions containing different levels of Pb^{2+} . For a level, a series of lead solutions with the same initial concentration

Fig. 3 SEM images of SBA-15/SH-5 (a), SBA-15/SH-10 (b), SBA-15/SH-15 (c), and SBA-15/SH-30 (d)

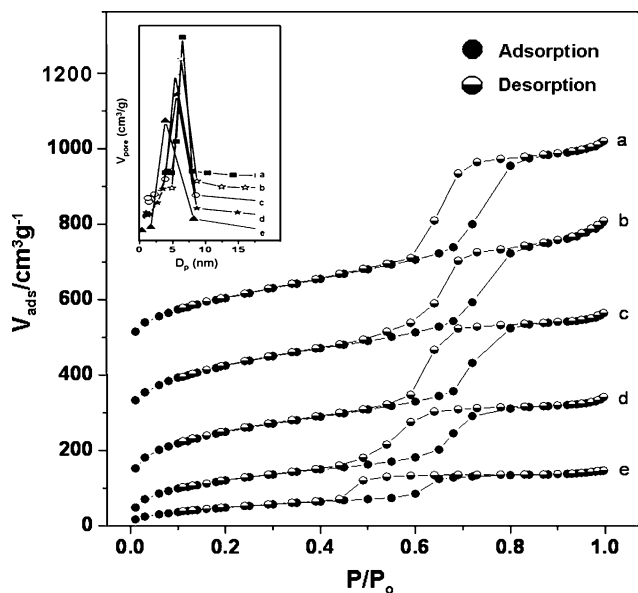
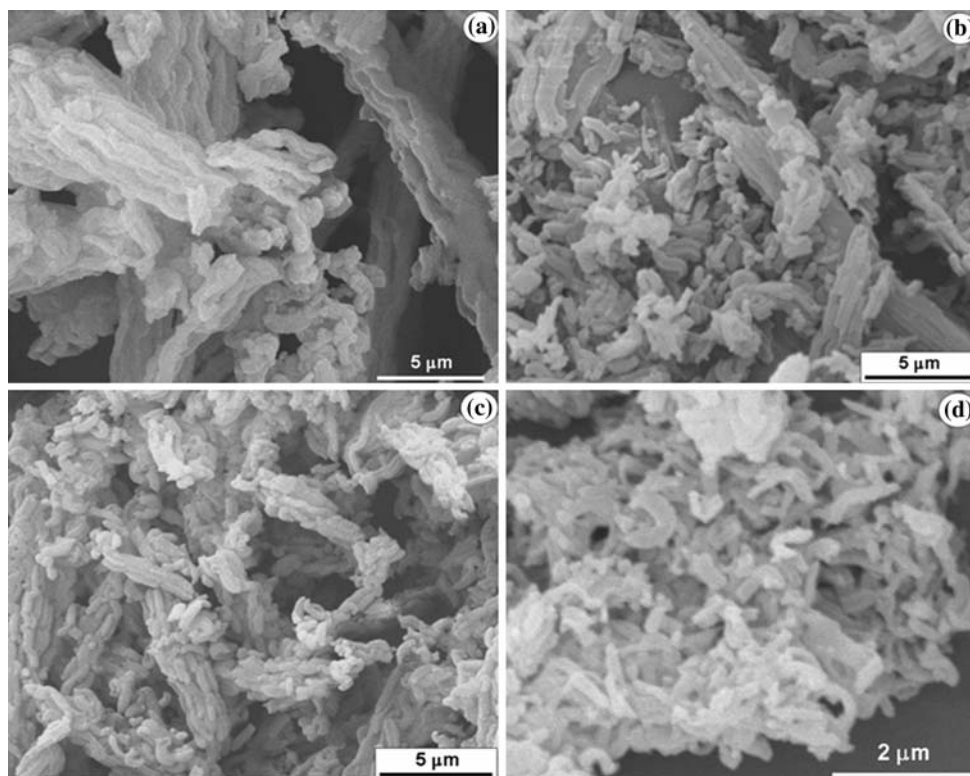


Fig. 4 N₂ adsorption–desorption isotherms and pore size distribution curves (the *inset*) of SBA-15/SH-5 (a), SBA-15/SH-10 (b), SBA-15/SH-15 (c), SBA-15/SH-20 (d), SBA-15/SH-30 (e)

were stirred in the presence of the adsorbent. Each solution was collected and analyzed at different times. This route was carried out for all of the SBA-15/SH-*x* materials. Figure 6 shows the result of a representative sample, SBA-15/SH-15, with initial Pb²⁺ concentration of 200 mg/L where the amount of lead (II) adsorbed increases with contact time, and

then attains equilibrium at about 90 min. Similar equilibrium times were obtained for the other materials in this work. Therefore, a stirring time of 120 min was selected for all of the subsequent adsorption experiments.

Adsorption isotherms

The isotherm for lead adsorption of SBA-15/SH-30 material is presented in Fig. 7. At low concentrations the isotherms were linear whereas they reach equilibrium at higher concentrations. The data for the adsorption were fitted to Langmuir isotherms and the Langmuir linear plot is shown in the inset of Fig. 7. The maximum adsorption capacity *Q*₀ was also calculated from the linearized Langmuir equation. The maximum adsorption capacities of 0.08, 0.11, 0.13, 0.15, and 0.19 mmol Pb/g for *x* = 5, 10, 15, 20, and 30 of SBA-15/SH-*x*, respectively, have been obtained. As expected, the maximum adsorption capacity of the different adsorbents steadily increases with their sulfur content.

Adsorption mechanism

To investigate adsorption mechanism, the initial and final pH values of aqueous solutions for all of the adsorption equilibrium experiments have been measured. For a representative material, SBA-15/SH-15, initial/final pHs of the solutions with initial concentrations of 50, 150, and

Fig. 5 IR spectrum of SBA-15/SH-5 (a), SBA-15/SH-10 (b), SBA-15/SH-15 (c), SBA-15/SH-20 (d), SBA-15/SH-30 (e) in the range of 400–4000 cm^{-1} and in 2400–2750 cm^{-1} (the inset)

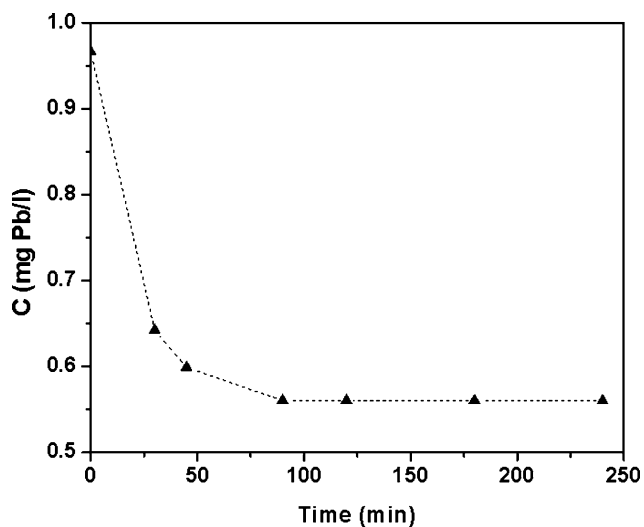
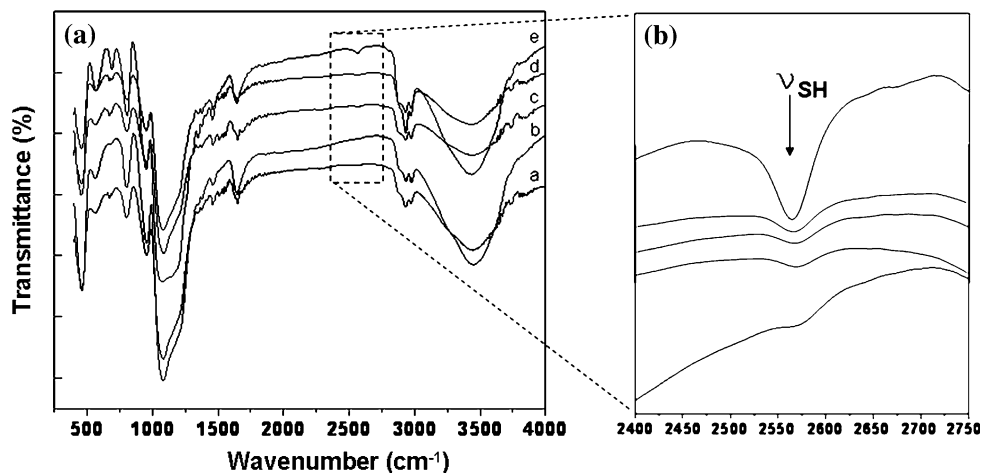


Fig. 6 Effect of contact time for the adsorption of lead(II) ions onto SBA-15/SH-15 with initial Pb^{2+} concentration of 200 mg/L at 30 °C

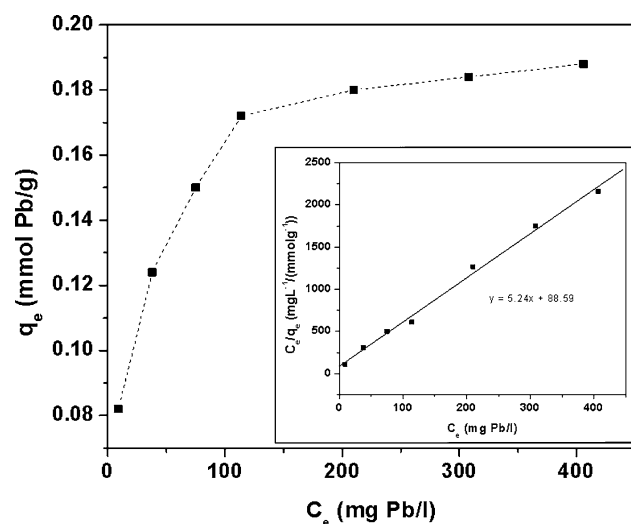
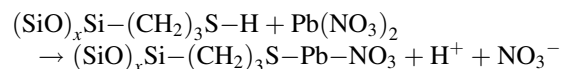


Fig. 7 The effect of initial concentrations and Langmuir plot (the inset) for the adsorption of lead(II) ions onto SBA-15/SH-30 at 30 °C

200 mg/L were 4.17/3.82, 4.07/3.55, and 3.96/3.46, respectively. Compared to the initial solution, a significant decrease of the final pH for the equilibrium solutions has been found. This pH decrease depends on the lead loading extent on the adsorbent, which agrees with the expected amount of protons released from the thiol groups. To clarify the chemical nature of the lead (II) species adsorbed on the SBA-15/SH- x materials, some samples were obtained by stirring 100 mg of each adsorbent in 50 mL of a 200 mg/L Pb(II) aqueous solution for 24 h. The lead-loaded solids were recovered by filtration, washed several times by water, dried at 100 °C for 1 h, and then analyzed by ICP. The result shows that molar ratio of sulfur, lead, and N were about 1:1:1. From this result, a proposed adsorption mechanism is that each lead atom is anchored to the sulfur of the thiol group and also bonded to a NO_3^- anion as follows.



Influence of the pH

It can be seen from the proposed mechanism above that proton concentration can modify the lead adsorption efficiency. Increasing proton concentration can lead to a decrease in content of lead-loaded component, which means that the adsorption decreases. The effect of the solution pH on the adsorption of lead (II) has been investigated for a representative adsorbent, SBA-15/SH-15. Isotherms have been obtained at selected pH values where lead species are in Pb^{2+} form in aqueous solution [34], and the results were shown in Fig. 8. As expected, a decrease in adsorption capacity with increasing proton concentration was obtained.

To reuse the adsorbent, an investigation on removal of lead on the lead-loaded solids was carried out. For this purpose, the lead-loaded solids were stirred in HCl

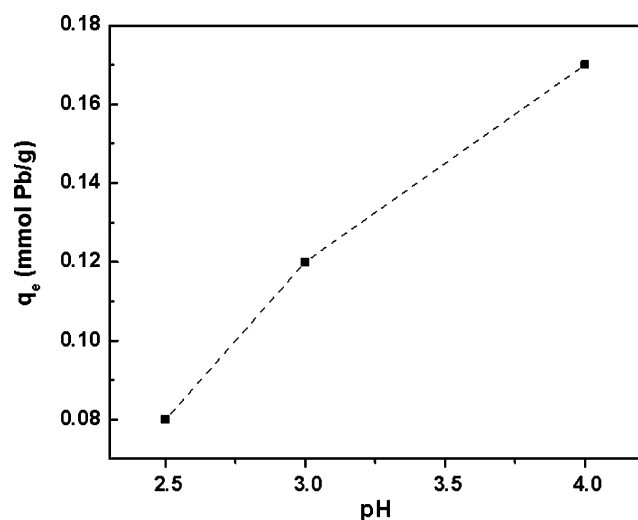


Fig. 8 Effect of pH for the adsorption of lead(II) ions onto SBA-15/SH-15 with initial Pb^{2+} concentration of 200 mg/L at 30 °C

solutions with different concentrations. The solid obtained by filtration, washed several times by water, dried at 100 °C, namely, lead-reloaded SBA-15/SH-*x*, were used in adsorption experiments. The results show that amount of lead desorbed increases with increasing proton concentration, and with the treatment in HCl 2 M solution, the adsorption efficiency of the lead-reloaded SBA-15/SH-15 sample can reach 80% after five cycles compared with the fresh SBA-15/SH-15 materials. The structure and thiol group of the materials remain after five cycles, which were evidenced by PXRD and IR (not shown). This result may support further potential application of this materials family in removal of lead ions in water.

Conclusion

The adsorption of lead from aqueous solutions on the thiol-functionalized SBA-15 materials with different thiol contents has been investigated. The lead adsorption approached equilibrium state in short time of about 90 min. The adsorption data have been fitted to Langmuir isotherms and a maximum lead loading of about 0.19 mmol Pb/g has been obtained for SBA-15/SH-30. This work also shows that the materials can be reused after adsorption by treatment of lead-loaded samples in HCl solutions with moderately high concentration.

Acknowledgement Financial support from the National Foundation for Science and Technology Development (NAFOSTED, 104.03.06.09) is gratefully acknowledged.

References

- Ake CL, Mayura K, Huebner H, Bratton GR, Philips TD (2001) *J Toxicol Environ Health A* 63:459
- Tunali S, Akar T, Ozcan AS, Kiran I, Ozcan A (2006) *Sep Purif Technol* 47:105
- Bektas N, Agim BA, Kara S (2004) *J Hazard Mater B* 112:115
- Ozcan AS, Gok O, Ozcan A (2009) *J Hazard Mater* 161:499
- Imamoglu M, Tekir O (2008) *Desalination* 228:108
- Moufih M, Alkik A, Sebti S (2005) *J Hazard Mater B* 119:183
- Qi L, Xu Z (2004) *Colloids Surf A Physicochem Eng Asp* 251:183
- Divya C, Nalini S (2008) *Bioresour Technol* 99:9021
- Sun QY, Yu P, Yang LZ (2004) *Environ Geochem Health* 26:311
- Ho YS, Ng JCY, McKay G (2001) *Sep Sci Technol* 36:241
- Yu B, Zhang Y, Shukla A, Shukla SS, Dorris KL (2001) *J Hazard Mater B* 84:83
- Rafatullaha M, Sulaiman O, Hashim R, Ahmad A (2009) *J Hazard Mater* 170:969
- Turkmenler H, Ozacar M, Sengil IA (2008) *Int J Environ Pollut* 33:212
- Zhan XM, Zhao X (2003) *Water Res* 37:3905
- Shrabani SM, Sujoy KD, Rajdeep C, Tapan S, Tara SB, Arun KG (2010) *Desalination* 251:96
- Liu SY, Gao J, Yang YJ, Yang YC, Ye ZX (2010) *J Hazard Mater* 173:558
- Benhima H, Chiban M, Sinan F, Seta P, Persin M (2008) *Colloids Surf B Biointerfaces* 61:10
- Wang LH, Lin CI (2008) *Ind Eng Chem Res* 47:4891
- Kresge CT, Leonowicz M, Roth WJ, Vartuli JC, Beck JC (1992) *Nature* 359:710
- Zhao D, Huo Q, Feng J, Chmelka BF, Stucky GD (1998) *J Am Chem Soc* 120:6024
- Lan X, Zhang W, Yan L, Ding Y, Han X, Lin L, Bao X (2009) *J Phys Chem C* 113:6589
- Tian BS, Yang C (2009) *J Phys Chem C* 113:4925
- Kadib AE, Hesemann P, Molvinger K, Brandner J, Biolley C, Gaveau P, Moreau JJE, Brunel D (2009) *J Am Chem Soc* 131:2882
- Lee B, Kim Y, Lee H, Yi J (2001) *Microporous Mesoporous Mater* 50:77
- Dai S, Burleigh MC, Ju YH, Gao HJ, Lin JS, Pennycook SJ, Barnes CE, Xue ZL (2000) *J Am Chem Soc* 122:992
- Brown J, Mercier L, Pinnavaia TJ (1999) *Chem Commun* 69
- Burleigh MC, Dai S, Hagaman EW, Lin LS (2001) *Chem Mater* 13:2537
- Liu AM, Hidajat K, Kawi S, Zhao DY (2000) *Chem Commun* 1145
- Jaroniec CP, Sayari A, Kruk M, Jaroniec M (1998) *J Phys Chem B* 102:5503
- Antochshuk V, Jaroniec M (1998) *J Phys Chem B* 103:6252
- Feng X, Fryxell GE, Wang LQ, Kim AY, Liu J, Kemner KM (1997) *Science* 276:923
- Beck JS, Vartuli JC, Roth WJ, Leonowicz ME, Kresge CT, Schmitt KD, Chu CTW, Olson DH, Scheppard EW, Mc Cullen CB, Higgins JB, Schlenker JL (1992) *J Am Chem Soc* 114:10834
- Chong ASM, Zhao XS (2003) *J Phys Chem B* 107:12650
- Xu D, Tan XL, Chen CL, Wang XK (2008) *Appl Clay Sci* 41:37